

DETERMINATION OF THE EQUIVALENT  
ANISOTROPY PROPERTIES OF POLYCRYSTALLINE

*Original*

DETERMINATION OF THE EQUIVALENT  
ANISOTROPY PROPERTIES OF POLYCRYSTALLINE

MAGNETIC MATERIALS: THEORETICAL

ASPECTS AND NUMERICAL ANALYSIS / Bottauscio, O.; CHIADO' PIAT, Valeria; Eleuteri, M.; Lussardi, L.; Manzin, A..  
- In: MATHEMATICAL MODELS AND METHODS IN APPLIED SCIENCES. - ISSN 0218-2025. - STAMPA. - 23:7(2013),  
pp. 1217-1233. [10.1142/S0218202513500073]

*Availability:*

This version is available at: 11583/2522375 since: 2019-02-11T15:17:07Z

*Publisher:*

World Scientific Publishing Company

*Published*

DOI:10.1142/S0218202513500073

*Terms of use:*

This article is made available under terms and conditions as specified in the corresponding bibliographic description in the repository

*Publisher copyright*

(Article begins on next page)

# DETERMINATION OF THE EQUIVALENT ANISOTROPY PROPERTIES OF POLYCRYSTALLINE MAGNETIC MATERIALS: THEORETICAL ASPECTS AND NUMERICAL ANALYSIS

O. BOTTAUSCIO, V. CHIADÒ PIAT, M. ELEUTERI, L. LUSSARDI, AND A. MANZIN

**ABSTRACT.** The aim of this paper is the determination of the equivalent anisotropy properties of polycrystalline magnetic materials, modeled as an assembly of monocrystalline grains with a stochastic spatial distribution of easy axes. The theory of  $\Gamma$ -convergence is here adopted to homogenize the anisotropic contribution in the energy functional and derive the equivalent anisotropy properties. The reliability of this approach is investigated focusing on the computation of the static hysteresis loops of polycrystalline magnetic thin films, starting from the numerical integration of the Landau-Lifshitz-Gilbert equation.

**Keywords:** Random anisotropy, Homogenization,  $\Gamma$ -convergence, Polycrystalline magnetic materials

**2010 Mathematics Subject Classification:** 49J45, 60H07.

## 1. INTRODUCTION

Micromagnetic numerical codes are nowadays a common tool for evaluating the magnetization processes arising in magnetic nanostructures ([1], [2], [3]). Their use allows a deep understanding of the relationships between structural properties and magnetic domain formation, with important outcomes in technological applications where the miniaturization of magnetic devices is fundamental.

Micromagnetics theory is based on a continuum approximation of the magnetization spatial distribution, where different energy contributions are competing to determine magnetic domain configuration ([1]). The contributions to the magnetic Gibbs free energy arise from the exchange, magnetostatic, anisotropy and Zeeman energies, whose accurate approximation is essential to correctly evaluate the time and spatial evolution of magnetization within the sample. Each energy term acts at a different spatial scale, from the nanometric resolution involved in the exchange term, to the sample dimensions for the long-range magnetostatic interactions. Magnetic anisotropy, which expresses the tendency of the magnetization to lie along certain crystallographic directions, plays its role at the intermediate level of grain dimensions. In particular, at this spatial scale, magnetic properties are influenced by the size, shape, boundary properties and orientation distribution of grains. Taking into account of all these aspects within micromagnetic simulations is a complex task, so that simulations are often performed under the hypothesis of single crystal, assuming uniaxial or cubic anisotropy. This assumption, valid for samples having dimensions comparable than grain size, becomes inadequate in the presence of polycrystalline materials, where the actual grain orientation and distribution affect the behavior of the entire system ([4], [5]).

Polycrystalline materials are usually modelled within micromagnetic numerical codes as an array of grains, geometrically constructed using Voronoi diagrams ([6], [7], [8], [9], [10], [11]). Each single-crystal grain is assumed to have a randomly oriented uniaxial anisotropy. This approach has a strong impact on the geometry building and meshing, making the pre-processing phase very complex.

In this paper we propose an alternative procedure, based on the replacement of the polycrystalline magnetic material with an homogenized sample having equivalent anisotropy properties. The magnetic medium is initially modeled as an assembly of monocrystalline grains, assuming a

stochastic spatial distribution of the easy axes and disregarding the effects due to grain boundaries and boundary imperfections. Then, the mathematical theory of  $\Gamma$ -convergence (for an exhaustive treatment see [12] and [13] for the application to homogenization) is applied to homogenize the anisotropic term in the Gibbs free energy. Finally, the equivalent anisotropy properties are determined and conveniently used in micromagnetic simulations, as recently shown in [14] for the computation of switching processes in polycrystalline magnetic films. The theory of  $\Gamma$ -convergence has been already applied in multiple-scale problems arising in micromagnetism, see for instance [15] and [16].

The paper is organized in four sections. The first one deals with the presentation of the main equations that govern the micromagnetic problem. The second one, devoted to the mathematical theory, provides the convergence result of the asymptotic problem and the relative proof. In the third one, the homogenization theory described in the previous section is applied to determine the equivalent anisotropy properties of an assembly of monocrystalline grains characterized by a stochastic distribution of the easy axes. In the last section, the result of the homogenization procedure is conveniently introduced in micromagnetic simulations, focusing on the computation of the static hysteresis loops of polycrystalline magnetic thin films. To put in evidence the limits of the proposed approach, the results obtained for homogenized samples are compared with those obtained by considering randomly distributed anisotropic properties.

## 2. SETTING OF THE PROBLEM

We deal with a polycrystalline magnetic sample, occupying a bounded open region  $D \subset \mathbb{R}^3$ . The system is characterized by a magnetization spatial distribution, defined by the magnetization vector field  $\mathbf{M} \in L^2(\mathbb{R}^3; \mathbb{R}^3)$  with  $|\mathbf{M}| = M_S \chi_D$  in  $\mathbb{R}^3$ , where the positive scalar constant  $M_S$  is the saturation magnetization. Let us denote by  $\mathbf{m} \in L^2(\mathbb{R}^3; \mathbb{R}^3)$  the rescaled magnetization  $\mathbf{m} = \mathbf{M}/M_S$ . In the presence of an externally applied magnetic field  $\mathbf{H}_a \in L^2(\mathbb{R}^3; \mathbb{R}^3)$ , the magnetic energy behavior is described by the following energy functional

$$(2.1) \quad F(\mathbf{m}, \mathbf{H}_a) = \int_D A |\nabla \mathbf{m}|^2 \, d\mathbf{x} + \int_D f_{\text{an}}(\mathbf{m}, \mathbf{u}_{\text{an}}) \, d\mathbf{x} - \frac{\mu_0}{2} \int_D M_S \mathbf{H}_m \cdot \mathbf{m} \, d\mathbf{x} - \mu_0 \int_D M_S \mathbf{H}_a \cdot \mathbf{m} \, d\mathbf{x}$$

where the four terms represent the exchange energy, the anisotropy energy, the magnetostatic energy and the Zeeman energy (i.e. the external field energy), respectively. In (2.1)  $\mu_0$  is the magnetic permeability of vacuum, the material parameter  $A$  is the exchange constant and the vector field  $\mathbf{H}_m$  is the magnetostatic field, expressed as a function of the magnetic scalar potential  $u$ , i.e.  $\mathbf{H}_m = \nabla u$ . In particular, the scalar potential  $u$  is the solution of the Poisson equation

$$(2.2) \quad \nabla^2 u + \nabla \cdot \mathbf{M} = 0 \quad \text{in } \mathbb{R}^3$$

complemented by appropriate boundary conditions on  $\partial D$ . The non negative function  $f_{\text{an}}$  represents the anisotropy energy density, which is typically a polynomial with symmetry properties influenced by the crystalline lattice microstructure. The minima of  $f_{\text{an}}$  correspond to the preferred directions of magnetization (i.e. easy axes). Under the hypothesis of uniaxial anisotropy (with easy axis defined by unit vector  $\mathbf{u}_{\text{an}}$ ), the anisotropy energy density is given by

$$(2.3) \quad f_{\text{an}}(\mathbf{m}, \mathbf{u}_{\text{an}}) = k_{\text{an}} [1 - (\mathbf{m} \cdot \mathbf{u}_{\text{an}})^2]$$

where  $k_{\text{an}}$  is the magnetocrystalline anisotropy constant. The polycrystalline magnetic material is here assumed as an assembly of monocrystalline grains with uniaxial anisotropy defined by the vector field  $\mathbf{u}_{\text{an}}$  and a fixed anisotropy constant  $k_{\text{an}}$  (see Fig. 1a).

Actually, we will consider a more general setting for the anisotropy energy function, i.e. we will take into account a stochastic distribution of easy axes. More precisely, if  $T$  is a 3-dimensional ergodic dynamical system on some probability space  $\Omega$  (see paragraph 3.1 for the precise mathematical definitions), then we let

$$(2.4) \quad f_{\text{an}}(\mathbf{m}, \mathbf{x}, \omega) = k_{\text{an}} [1 - (\mathbf{m} \cdot \mathbf{u}_{\text{an}}(T_{\mathbf{x}}\omega))^2]$$

being  $\mathbf{u}_{\text{an}}: \Omega \rightarrow \mathbb{R}^3$  and  $|\mathbf{u}_{\text{an}}(\omega)| = 1$  a.s. in  $\Omega$ .

By introducing the scale parameter  $\varepsilon$  that correlates microscopic and macroscopic spatial cases, the energy functional of the magnetic material is then defined by

$$(2.5) \quad F_\varepsilon(\mathbf{m}, \omega) = \int_D A |\nabla \mathbf{m}|^2 \, d\mathbf{x} + \int_D f_{\text{an}}\left(\mathbf{m}, \frac{\mathbf{x}}{\varepsilon}, \omega\right) \, d\mathbf{x} - \frac{\mu_0}{2} \int_D M_S \mathbf{H}_m \cdot \mathbf{m} \, d\mathbf{x} - \mu_0 \int_D M_S \mathbf{H}_a \cdot \mathbf{m} \, d\mathbf{x}.$$

Our purpose is the study of the limit, as  $\varepsilon \rightarrow 0$ , of the energy functional (2.5), by means of the theory of  $\Gamma$ -convergence.

### 3. HOMOGENIZATION RESULT

**3.1. Some preliminary notions.** Let  $(\Omega, \mathcal{F}, \mu)$  be a probability space, where  $\mathcal{F}$  is a  $\sigma$ -algebra of subsets of  $\Omega$  and  $\mu$  is a probability measure on  $\Omega$ .

Let  $n \in \mathbb{N}$  with  $n \geq 1$ . A  $n$ -dimensional dynamical system  $T$  on  $\Omega$  is a family of mappings

$$T_{\mathbf{x}}: \Omega \rightarrow \Omega, \quad \mathbf{x} \in \mathbb{R}^n$$

such that

- a)  $T_0 = \text{Id}$  and  $T_{\mathbf{x}+\mathbf{y}} = T_{\mathbf{x}}T_{\mathbf{y}}$  for any  $\mathbf{x}, \mathbf{y} \in \mathbb{R}^n$ .
- b) For every  $\mathbf{x} \in \mathbb{R}^n$  and every set  $E \in \mathcal{F}$  we have

$$T_{\mathbf{x}}E \in \mathcal{F} \quad \text{and} \quad \mu(T_{\mathbf{x}}E) = \mu(E).$$

- c) For any measurable function  $f: \Omega \rightarrow \mathbb{R}^m$ , the function  $\tilde{f}: \mathbb{R}^n \times \Omega \rightarrow \mathbb{R}^m$  given by

$$\tilde{f}(\mathbf{x}, \omega) = f(T_{\mathbf{x}}\omega)$$

is measurable.

Given a  $n$ -dimensional dynamical system  $T$  on  $\Omega$ , a measurable function  $f$  defined on  $\Omega$  is said to be *invariant* if  $f(T_{\mathbf{x}}\omega) = f(\omega)$  a.s. in  $\Omega$ , for each  $\mathbf{x} \in \mathbb{R}^n$ ; a dynamical system is said to be *ergodic* if the only invariant functions are the constants.

The *expected value* of a random variable  $f: \Omega \rightarrow \mathbb{R}^m$  is defined as

$$\mathbb{E}(f) = \int_{\Omega} f(\omega) \, d\mu(\omega).$$

The most important result we need is the following Theorem.

**Theorem 3.1. (Birkhoff's Ergodic Theorem)** *Let  $m \in \mathbb{N}$  with  $m \geq 1$ , let  $f \in L^1(\Omega; \mathbb{R}^m)$  and  $T$  be a  $n$ -dimensional ergodic dynamical system on  $\Omega$ . Then, it holds*

$$\mathbb{E}(f) = \lim_{r \rightarrow 0} \frac{1}{|K|} \int_K f(T_{\frac{\mathbf{x}}{r}}\omega) \, d\mathbf{x}, \quad \text{a.s. in } \Omega$$

for any  $K \subset \mathbb{R}^n$  bounded, measurable, with  $|K| > 0$  (here, and in what follows,  $|A|$  denotes the Lebesgue measure of  $A \subset \mathbb{R}^n$ , with  $A$  measurable).

Let  $X: \Omega \rightarrow \mathbb{R}^n$  be a random variable, i.e.  $X$  is a measurable map. Then, it is possible to construct, in a canonical way, a Borel measure on  $\mathbb{R}^n$ , called *law* or *distribution* of  $X$ , given by

$$(3.1) \quad \mu_X(B) = \mu(X^{-1}(B)), \quad \text{for any } B \text{ Borel in } \mathbb{R}^n.$$

If we assume that  $\mu_X = \rho \, d\mathcal{L}^n$ , with

$$\rho(\mathbf{x}) = \frac{1}{s\sqrt{2\pi}} \exp\left(\frac{-|\mathbf{x} - \eta|^2}{2s^2}\right), \quad s > 0,$$

then  $X$  is said to be a *Gaussian* random variable with *standard deviation*  $s$  and *expected value*  $\eta$ .

**3.2. The  $\Gamma$ -convergence result.** In this paragraph we investigate the homogenization problem by a purely mathematical point of view; in the next paragraph we will apply the general convergence Theorem 3.2 to the physical situation we are interested.

Let  $D$  be a bounded open subset in  $\mathbb{R}^3$ ,  $c_1, c_2, c_3 > 0$  given constants and  $\mathbf{H} \in L^2(\mathbb{R}^3; \mathbb{R}^3)$ . Let us denote by  $K$  the set of all vector fields  $\mathbf{m} \in L^2(\mathbb{R}^3; \mathbb{R}^3)$  with  $\mathbf{m}|_D \in H^1(D; \mathbb{R}^3)$  and  $|\mathbf{m}| = \chi_D$  a.e. in  $\mathbb{R}^3$ . For any  $\mathbf{m} \in K$  let us denote by  $v \in H^1(\mathbb{R}^3)$  the solution of the equation

$$(3.2) \quad \nabla^2 v + \nabla \cdot \mathbf{m} = 0, \text{ in } \mathcal{D}'(\mathbb{R}^3).$$

(see for instance [17] for details on existence and uniqueness).

Let  $(\Omega, \mathcal{F}, \mu)$  be a probability space and  $T$  be a 3-dimensional ergodic dynamical system on  $\Omega$ . Let  $\varphi: \mathbb{R}^3 \times \mathbb{R}^3 \times \Omega \rightarrow [0, +\infty)$  be a measurable map such that  $\varphi(0, 0, \cdot) \in L^1(\Omega)$  and

$$(3.3) \quad |\varphi(\mathbf{m}_1, \mathbf{x}, \omega) - \varphi(\mathbf{m}_2, \mathbf{x}, \omega)| \leq L|\mathbf{m}_1 - \mathbf{m}_2|$$

for some constant  $L > 0$ , for all  $(\mathbf{x}, \omega) \in \mathbb{R}^3 \times \Omega$  and for any  $\mathbf{m}_1, \mathbf{m}_2 \in \mathbb{R}^3$ . Moreover, we assume that for any  $\mathbf{m} \in \mathbb{R}^3$  the random field  $\varphi(\mathbf{m}, \cdot, \cdot)$  is stationary and ergodic: therefore,  $\varphi(\mathbf{m}, \mathbf{x}, \omega) = f(\mathbf{m}, T_{\mathbf{x}}\omega)$  for a suitable map  $f: \mathbb{R}^3 \times \Omega \rightarrow [0, +\infty)$ .

For any  $\varepsilon > 0$  and any  $\omega \in \Omega$  let  $E_\varepsilon(\cdot, \omega): L^2(\mathbb{R}^3; \mathbb{R}^3) \rightarrow [0, +\infty]$  be defined by

$$E_\varepsilon(\mathbf{m}, \omega) := \begin{cases} c_1 \int_D |\nabla \mathbf{m}|^2 d\mathbf{x} + \int_D f(\mathbf{m}, T_{\frac{\mathbf{x}}{\varepsilon}}\omega) d\mathbf{x} + c_2 \int_{\mathbb{R}^3} |\nabla v|^2 d\mathbf{x} - c_3 \int_D \mathbf{H} \cdot \mathbf{m} d\mathbf{x} & \text{if } \mathbf{m} \in K \\ +\infty & \text{otherwise.} \end{cases}$$

We are ready to state the main result of this section.

**Theorem 3.2.** *The family  $(E_\varepsilon(\cdot, \omega))_{\varepsilon > 0}$   $\Gamma$ -converges, a.s. in  $\Omega$  as  $\varepsilon \rightarrow 0^+$ , with respect to the strong topology of  $L^2(\mathbb{R}^3; \mathbb{R}^3)$ , to the functional  $\bar{E}: L^2(\mathbb{R}^3; \mathbb{R}^3) \rightarrow [0, +\infty]$  given by*

$$\bar{E}(\mathbf{m}) := \begin{cases} c_1 \int_D |\nabla \mathbf{m}|^2 d\mathbf{x} + \int_D \bar{f}(\mathbf{m}(\mathbf{x})) d\mathbf{x} + c_2 \int_{\mathbb{R}^3} |\nabla v|^2 d\mathbf{x} - c_3 \int_D \mathbf{H} \cdot \mathbf{m} d\mathbf{x} & \text{if } \mathbf{m} \in K \\ +\infty & \text{otherwise.} \end{cases}$$

where

$$\bar{f}(\mathbf{m}) := \int_{\Omega} f(\omega, \mathbf{m}) d\mu(\omega), \quad \forall \mathbf{m} \in \mathbb{R}^3.$$

*Proof.* Let us fix a positive infinitesimal sequence  $(\varepsilon_j)$ .

*Step 1:* We prove that if  $\mathbf{m}_j \rightarrow \mathbf{m}$  in  $L^2(\mathbb{R}^3; \mathbb{R}^3)$  and  $E_{\varepsilon_j}(\mathbf{m}_j, \omega) \leq M$ , for some  $M \geq 0$ , if necessary depending on  $\omega$ , then, up to subsequences,  $\mathbf{m}_j|_D \rightarrow \mathbf{m}|_D$  weakly in  $H^1(D; \mathbb{R}^3)$  and  $\mathbf{m} \in K$ .

By Hölder inequality we have

$$c_1 \int_D |\nabla \mathbf{m}_j|^2 d\mathbf{x} \leq M + c_3 \int_D \mathbf{H} \cdot \mathbf{m}_j d\mathbf{x} \leq M + \|\mathbf{H}\|_{L^2(\mathbb{R}^3; \mathbb{R}^3)} \|\mathbf{m}_j\|_{L^2(\mathbb{R}^3; \mathbb{R}^3)}.$$

Then  $\|\nabla \mathbf{m}_j\|_{L^2(D; \mathbb{R}^3)}$  is bounded, and thus  $\mathbf{m}_j|_D \rightarrow \mathbf{m}|_D$  weakly in  $H^1(D; \mathbb{R}^3)$ , since  $\mathbf{m}_j = \mathbf{m} = 0$  a.e. in  $\mathbb{R}^3 \setminus D$ . Obviously we also obtain  $\mathbf{m}|_D \in H^1(D; \mathbb{R}^3)$ , and then  $\mathbf{m} \in K$ .

*Step 2:* Let  $\mathbf{m}_j \rightarrow \mathbf{m}$  in  $L^2(\mathbb{R}^3; \mathbb{R}^3)$ , and let  $v_j, v \in H^1(\mathbb{R}^3)$  be such that

$$(3.4) \quad \nabla^2 v_j + \nabla \cdot \mathbf{m}_j = \nabla^2 v + \nabla \cdot \mathbf{m} = 0, \quad \text{in } \mathcal{D}'(\mathbb{R}^3).$$

We claim that  $v_j \rightarrow v$  weakly in  $H_{\text{loc}}^1(\mathbb{R}^3)$ .

Indeed, equation (3.4) means

$$(3.5) \quad \int_{\mathbb{R}^3} \nabla v_j \cdot \nabla \psi \, d\mathbf{x} + \int_{\mathbb{R}^3} \mathbf{m}_j \cdot \nabla \psi \, d\mathbf{x} = 0, \quad \forall \psi \in H^1(\mathbb{R}^3).$$

Letting  $\psi = v_j$  in (3.5) we get

$$- \int_{\mathbb{R}^3} |\nabla v_j|^2 \, d\mathbf{x} - \int_{\mathbb{R}^3} \mathbf{m}_j \cdot \nabla v_j \, d\mathbf{x} = 0.$$

Taking into account Hölder inequality we deduce that

$$\int_{\mathbb{R}^3} |\nabla v_j|^2 \, d\mathbf{x} \leq \|\nabla v_j\|_{L^2(\mathbb{R}^3)} \|\mathbf{m}_j\|_{L^2(\mathbb{R}^3; \mathbb{R}^3)}$$

and then  $\nabla v_j$  is equibounded in  $L^2(\mathbb{R}^3)$ . By the Sobolev-Gagliardo-Nirenberg inequality we have

$$\|v_j\|_{L^6(\mathbb{R}^3)} \leq C \|\nabla v_j\|_{L^2(\mathbb{R}^3)}$$

for some constant  $C > 0$ . Then the sequence  $(v_j)$  is bounded also in  $L^2_{\text{loc}}(\mathbb{R}^3)$ , which implies that, up to a subsequence,  $v_j \rightarrow w$  weakly in  $H^1_{\text{loc}}(\mathbb{R}^3)$ . Now passing to the limit as  $j \rightarrow +\infty$  in (3.5) we deduce that

$$\int_{\mathbb{R}^3} \nabla w \cdot \nabla \psi \, d\mathbf{x} + \int_{\mathbb{R}^3} \mathbf{m} \cdot \nabla \psi \, d\mathbf{x} = 0, \quad \forall \psi \in H^1(\mathbb{R}^3)$$

and then  $\nabla^2 w + \nabla \cdot \mathbf{m} = 0$  in  $\mathcal{D}'(\mathbb{R}^3)$ . This also yields that  $w \in H^1(\mathbb{R}^3)$ , and thus  $w = v$ .

*Step 3:* We prove the  $\Gamma$ -lim inf inequality, i.e. for any sequence  $\mathbf{m}_j \rightarrow \mathbf{m}$  in  $L^2(\mathbb{R}^3; \mathbb{R}^3)$  we have

$$(3.6) \quad \liminf_{j \rightarrow +\infty} E_{\varepsilon_j}(\mathbf{m}_j, \omega) \geq \bar{E}(\mathbf{m}) \quad \text{a.s. in } \Omega.$$

Since  $\mathbf{m}_j|_D \rightarrow \mathbf{m}|_D$  weakly in  $H^1(D; \mathbb{R}^3)$ , by step 1, and since  $\nabla v_j \rightharpoonup \nabla v$  weakly in  $L^2(\mathbb{R}^3; \mathbb{R}^3)$ , by step 2, from lower semicontinuity we have

$$(3.7) \quad \begin{aligned} \liminf_{j \rightarrow +\infty} \left( c_1 \int_D |\nabla \mathbf{m}_j|^2 \, d\mathbf{x} + c_2 \int_{\mathbb{R}^3} |\nabla v_j|^2 \, d\mathbf{x} - c_3 \int_D \mathbf{H} \cdot \mathbf{m}_j \, d\mathbf{x} \right) &\geq \\ &\geq c_1 \int_D |\nabla \mathbf{m}|^2 \, d\mathbf{x} + c_2 \int_{\mathbb{R}^3} |\nabla v|^2 \, d\mathbf{x} - c_3 \int_D \mathbf{H} \cdot \mathbf{m} \, d\mathbf{x}. \end{aligned}$$

Now we show that

$$(3.8) \quad \lim_{j \rightarrow +\infty} \int_D f(\mathbf{m}_j(\mathbf{x}), T_{\frac{\mathbf{x}}{\varepsilon_j}} \omega) \, d\mathbf{x} = \int_D \int_{\Omega} f(\mathbf{m}(\mathbf{x}), \omega) \, d\mu(\omega) \, d\mathbf{x}.$$

Using (3.3) and Hölder inequality we get

$$\left| \int_D f(\mathbf{m}_j(\mathbf{x}), T_{\frac{\mathbf{x}}{\varepsilon_j}} \omega) \, d\mathbf{x} - \int_D f(\mathbf{m}(\mathbf{x}), T_{\frac{\mathbf{x}}{\varepsilon_j}} \omega) \, d\mathbf{x} \right| \leq L \int_D |\mathbf{m}_j - \mathbf{m}| \, d\mathbf{x} \leq L \sqrt{|D|} \|\mathbf{m}_j - \mathbf{m}\|_{L^2(D; \mathbb{R}^3)}$$

and then

$$\left| \int_D f(\mathbf{m}_j(\mathbf{x}), T_{\frac{\mathbf{x}}{\varepsilon_j}} \omega) \, d\mathbf{x} - \int_D f(\mathbf{m}(\mathbf{x}), T_{\frac{\mathbf{x}}{\varepsilon_j}} \omega) \, d\mathbf{x} \right| \rightarrow 0.$$

Hence, in order to prove (3.8) it suffices to show that

$$(3.9) \quad \lim_{j \rightarrow +\infty} \int_D f(\mathbf{m}(\mathbf{x}), T_{\frac{\mathbf{x}}{\varepsilon_j}} \omega) \, d\mathbf{x} = \int_D \int_{\Omega} f(\mathbf{m}(\mathbf{x}), \omega) \, d\mu(\omega) \, d\mathbf{x}.$$

Let  $(D_h)_{h=1, \dots, M}$  be a partition of  $D$  and  $\mathbf{m}_h \in \mathbb{R}^3$  be such that  $\sum_{h=1}^M \mathbf{m}_h \chi_{D_h}$  tends to  $\mathbf{m}$  in  $L^1(D)$  as  $M \rightarrow +\infty$  and

$$(3.10) \quad \lim_{M \rightarrow +\infty} \sum_{h=1}^M |D_h| \int_{\Omega} f(\mathbf{m}_h, \omega) \, d\mu(\omega) = \int_D \int_{\Omega} f(\mathbf{m}(\mathbf{x}), \omega) \, d\mu(\omega) \, d\mathbf{x}.$$

For any  $h = 1, \dots, M$  we have, by Theorem 3.1,

$$\int_{D_h} f(\mathbf{m}_h, T_{\frac{\mathbf{x}}{\varepsilon_j}} \omega) \, d\mathbf{x} = |D_h| \frac{1}{|D_h|} \int_{D_h} f(\mathbf{m}_h, T_{\frac{\mathbf{x}}{\varepsilon_j}} \omega) \, d\mathbf{x} \xrightarrow{j \rightarrow +\infty} |D_h| \int_{\Omega} f(\mathbf{m}_h, \omega) \, d\mu(\omega).$$

Moreover, from the Lipschitz-continuity of  $f(\cdot, \omega)$ , we have that,

$$(3.11) \quad \left| \int_D f(\mathbf{m}(\mathbf{x}), T_{\frac{\mathbf{x}}{\varepsilon_j}} \omega) d\mathbf{x} - \int_D f\left(\sum_{h=1}^M \mathbf{m}_h \chi_{D_h}(\mathbf{x}), T_{\frac{\mathbf{x}}{\varepsilon_j}} \omega\right) d\mathbf{x} \right| \leq L \left\| m - \sum_{h=1}^M \mathbf{m}_h \chi_{D_h} \right\|_{L^1(D)}.$$

Now using (3.10), (3.11) we obtain (3.9), hence (3.8). Combining (3.7) with (3.8) we obtain the  $\Gamma$ -lim inf inequality (3.6).

*Step 4:* We prove the  $\Gamma$ -limsup inequality, i.e. for any  $\mathbf{m} \in L^2(\mathbb{R}^3; \mathbb{R}^3)$  there exists a sequence  $(\mathbf{m}_j)$  with  $\mathbf{m}_j \rightarrow \mathbf{m}$  strongly in  $L^2(\mathbb{R}^3; \mathbb{R}^3)$  such that

$$\limsup_{j \rightarrow +\infty} E_{\varepsilon_j}(\mathbf{m}_j, \omega) \leq \bar{E}(\mathbf{m}), \quad \text{a.s. in } \Omega.$$

To do this it suffices to observe that for each  $\mathbf{m} \in L^2(\mathbb{R}^3; \mathbb{R}^3)$  it holds

$$\lim_{j \rightarrow +\infty} E_{\varepsilon_j}(\mathbf{m}, \omega) = \bar{E}(\mathbf{m}) \quad \text{a.s. in } \Omega,$$

and this yields the conclusion.  $\square$

**3.3. Application to polycrystalline magnetic materials.** Here we refer to the notation introduced in the paragraph 3.2. Let  $M_S > 0$  be a constant and for any  $\mathbf{m} \in K$  let  $\mathbf{H}_m := \nabla u$ , where  $u := M_S v$  and  $v \in H^1(\mathbb{R}^3)$  is the solution of equation (3.2). Then, if  $\mathbf{M} := M_S \mathbf{m}$  we get

$$\nabla^2 u + \nabla \cdot \mathbf{M} = 0, \quad \text{in } \mathcal{D}'(\mathbb{R}^3).$$

Moreover, we deduce that, by divergence Theorem,

$$(3.12) \quad \int_{\mathbb{R}^3} |\nabla v|^2 d\mathbf{x} = - \int_{\mathbb{R}^3} \nabla v \cdot \mathbf{m} d\mathbf{x} = - \frac{1}{M_S} \int_{\mathbb{R}^3} \mathbf{H}_m \cdot \mathbf{m} d\mathbf{x} = - \frac{1}{M_S} \int_D \mathbf{H}_m \cdot \mathbf{m} d\mathbf{x}.$$

Let  $A, \mu_0 > 0$  be given constants. Let  $\mathbf{u}_{\text{an}}: \Omega \rightarrow \mathbb{R}^3$  be measurable such that  $|\mathbf{u}_{\text{an}}(\omega)| = 1$  a.s. in  $\Omega$ . Let  $k_{\text{an}} > 0$  be fixed and let  $f_{\text{an}}: \mathbb{R}^3 \times \mathbb{R}^3 \times \Omega \rightarrow [0, +\infty)$  be the anisotropy function given by (2.4). Finally, fix  $\mathbf{H}_a \in L^2(\mathbb{R}^3; \mathbb{R}^3)$ .

For any  $\varepsilon > 0$  and  $\omega \in \Omega$  let  $F_\varepsilon(\cdot, \omega): L^2(\mathbb{R}^3; \mathbb{R}^3) \rightarrow [0, +\infty]$  be defined as in (2.5), if  $\mathbf{m} \in K$ , and  $F_\varepsilon(\mathbf{m}, \omega) = +\infty$  otherwise in  $L^2(\mathbb{R}^3; \mathbb{R}^3)$ . Then, taking into account (3.12) we can apply Theorem 3.2 with the choice

$$c_1 := A, \quad c_2 := \frac{\mu_0 M_S^2}{2}, \quad c_3 := \mu_0 M_S, \quad \mathbf{H} := \mathbf{H}_a, \quad \varphi := f_{\text{an}}$$

and we obtain the following Theorem:

**Theorem 3.3.** *The family  $(F_\varepsilon(\cdot, \omega))_{\varepsilon > 0}$   $\Gamma$ -converges, as  $\varepsilon \rightarrow 0^+$ , with respect to the strong topology of  $L^2(\mathbb{R}^3; \mathbb{R}^3)$  and a.s. in  $\Omega$ , to the functional  $\bar{F}: L^2(\mathbb{R}^3; \mathbb{R}^3) \rightarrow [0, +\infty]$  given by*

$$\bar{F}(\mathbf{m}) := \begin{cases} \int_D A |\nabla \mathbf{m}|^2 d\mathbf{x} + \int_D \bar{f}_{\text{an}}(\mathbf{m}(\mathbf{x})) d\mathbf{x} - \frac{\mu_0}{2} \int_D M_S \mathbf{H}_m \cdot \mathbf{m} d\mathbf{x} - \mu_0 \int_D M_S \mathbf{H}_a \cdot \mathbf{m} d\mathbf{x} & \text{if } \mathbf{m} \in K \\ +\infty & \text{otherwise in } L^2(\mathbb{R}^3; \mathbb{R}^3) \end{cases}$$

where  $\bar{f}_{\text{an}}: \mathbb{R}^3 \rightarrow [0, +\infty)$  is given by

$$\bar{f}_{\text{an}}(\mathbf{m}) = k_{\text{an}} \int_{\Omega} [1 - (\mathbf{m} \cdot \mathbf{u}_{\text{an}}(\omega))^2] d\mu(\omega).$$

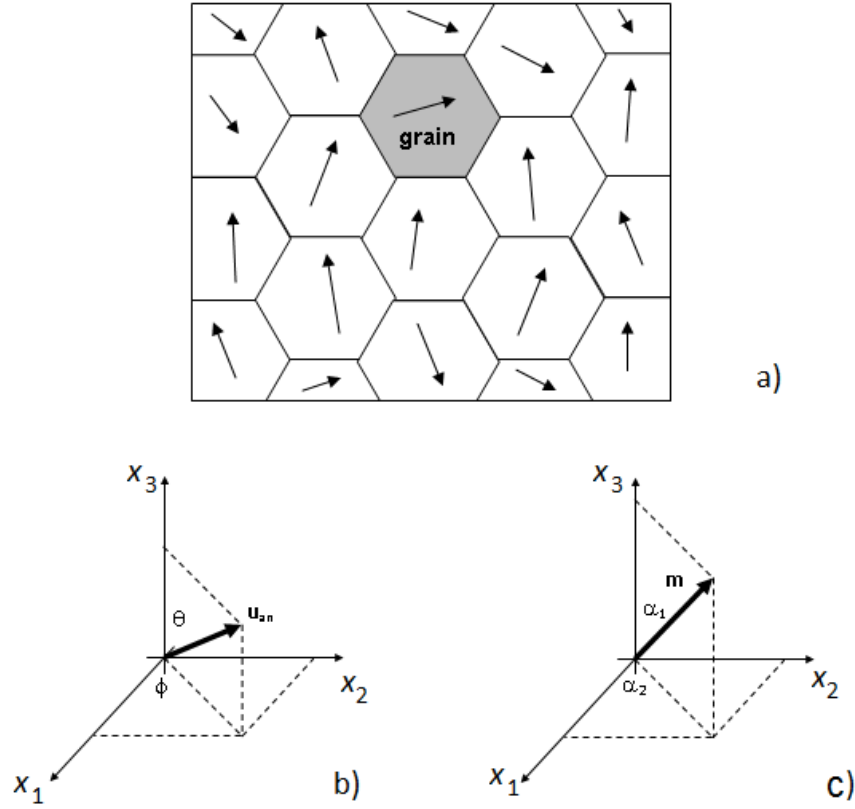


FIGURE 1. Schematic representation of the polycrystalline sample (a) and definition of local spherical coordinate systems for  $\mathbf{u}_{\text{an}}$  (b) and  $\mathbf{m}$  (c).

#### 4. DETERMINATION OF EQUIVALENT ANISOTROPY PROPERTIES

In this section the result of the asymptotic problem is applied to the calculation of the equivalent anisotropy properties of a polycrystalline magnetic sample, considering a uniform spatial distribution of the magnetization vector: such a sample is represented as an assembly of grains characterized by a random distribution of easy axes (Fig. 1a).

By introducing a spherical coordinate system (Fig. 1b) with angular coordinates  $\theta$  ( $0 \leq \theta \leq \pi$ ) and  $\phi$  ( $0 \leq \phi \leq 2\pi$ ), the anisotropy vector  $\mathbf{u}_{\text{an}}: \Omega \rightarrow \mathbb{R}^3$  is expressed as

$$(4.1) \quad \mathbf{u}_{\text{an}} = \sin \theta \cos \phi \mathbf{i}_1 + \sin \theta \sin \phi \mathbf{i}_2 + \cos \theta \mathbf{i}_3.$$

Vector  $\mathbf{u}_{\text{an}}$  is assumed to be a Gaussian random variable, with a probability density function  $P(\theta, \phi) = \rho(\theta)\rho(\phi)$  where

$$(4.2) \quad \rho(\nu) = \frac{1}{s_\nu \sqrt{2\pi}} \exp\left(-\frac{|\nu - \eta_\nu|^2}{2s_\nu^2}\right).$$

In (4.2)  $\nu = \theta$  (or  $\nu = \phi$ ),  $s_\nu$  is the standard deviation and  $\eta_\nu$  is the expected value.

Having assigned to  $\mathbf{m}$  a specific direction described by angles  $\alpha_1$  ( $0 \leq \alpha_1 \leq \pi$ ) and  $\alpha_2$  ( $0 \leq \alpha_2 \leq 2\pi$ ), indicated in Fig. 1c, the equivalent anisotropy function  $\bar{f}_{\text{an}}(\mathbf{m})$  is numerically computed



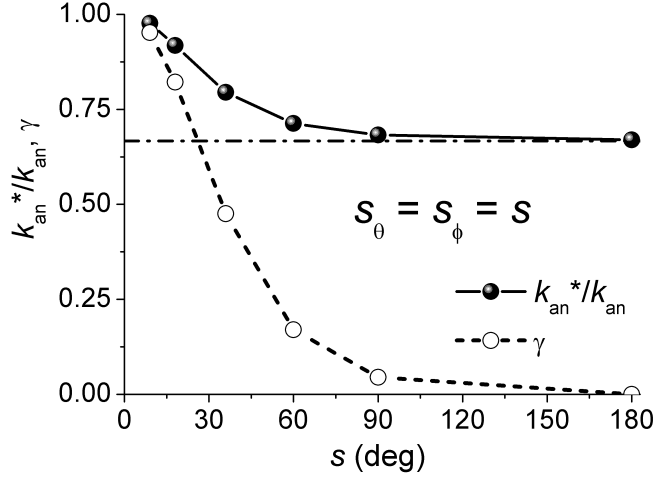


FIGURE 2. Asymptotic behaviour of the equivalent parameters  $k_{an}^*$  and  $\gamma$  at the increase of the standard deviation  $s$ , having assumed  $\eta_\theta = \pi/2$  and  $\eta_\phi = 0$ . The interpolation is made under the hypothesis of equivalent unidirectional anisotropy, by using the interpolating function defined in (4.4).

as:

$$(4.3) \quad \bar{f}_{an}(\mathbf{m}) = \bar{f}_{an}(\alpha_1, \alpha_2) = \frac{1}{\int_0^\pi \int_0^{2\pi} P(\theta, \phi) \sin \theta \, d\theta \, d\phi} \int_0^\pi \int_0^{2\pi} f_{an}(\mathbf{m}, \mathbf{u}_{an}) P(\theta, \phi) \sin \theta \, d\theta \, d\phi$$

where

$$f_{an}(\mathbf{m}, \mathbf{u}_{an}) = f_{an}(\alpha_1, \alpha_2, \theta, \phi) = k_{an}[1 - (\mathbf{m}(\alpha_1, \alpha_2) \cdot \mathbf{u}_{an}(\theta, \phi))^2].$$

In order to derive equivalent anisotropy parameters,  $\bar{f}_{an}(\mathbf{m})$  is numerically interpolated by an equivalent unidirectional anisotropy function having the following form

$$(4.4) \quad f_{an}^*(\mathbf{m}) = k_{an}^*[1 - \gamma(\mathbf{m} \cdot \mathbf{u}_{an}(\eta_\theta, \eta_\phi))^2]$$

where  $k_{an}^*$  is the equivalent anisotropy constant and  $\gamma$  is a dimensionless interpolating coefficient.

An example of the asymptotic behavior of parameters  $k_{an}^*$  and  $\gamma$  at the increase of the standard deviation  $s$ , here assumed identical for the two angular coordinates (that is  $s = s_\theta = s_\phi$ ), is shown in Fig. 2, having assumed  $\eta_\theta = \pi/2$  and  $\eta_\phi = 0$ .

In the case of uniform distribution of vector  $\mathbf{u}_{an}$  in the  $(x_1, x_2)$ -plane, the following equivalent planar anisotropy function is used as interpolator:

$$(4.5) \quad f_{an}^*(\mathbf{m}) = k_{an}^*[1 - \gamma(\mathbf{m}_{x_1} \mathbf{u}_{an, x_1}(\eta_\theta) + \mathbf{m}_{x_2} \mathbf{u}_{an, x_2}(\eta_\phi))^2].$$

In Fig. 3 we have reported the plots of the equivalent anisotropy functions and of the corresponding energy surfaces for Gaussian distribution with  $s = \pi/6$  (a) and for uniform distribution (b).

## 5. APPLICATION OF THE HOMOGENIZATION RESULT

The homogenization procedure described in the previous sections is applied to the computation of the static hysteresis loop of a thin film made of a polycrystalline magnetic material. The film, having planar size equal to  $2 \mu\text{m} \times 2 \mu\text{m}$  and thickness of 20 nm, is assumed to have a distribution of grains in the  $(x_1, x_2)$ -plane, with square shape and dimension equal to 20 nm or 100 nm. Each grain is associated to a given anisotropy direction  $\mathbf{u}_{an}$ , which is randomly distributed over the entire sample.

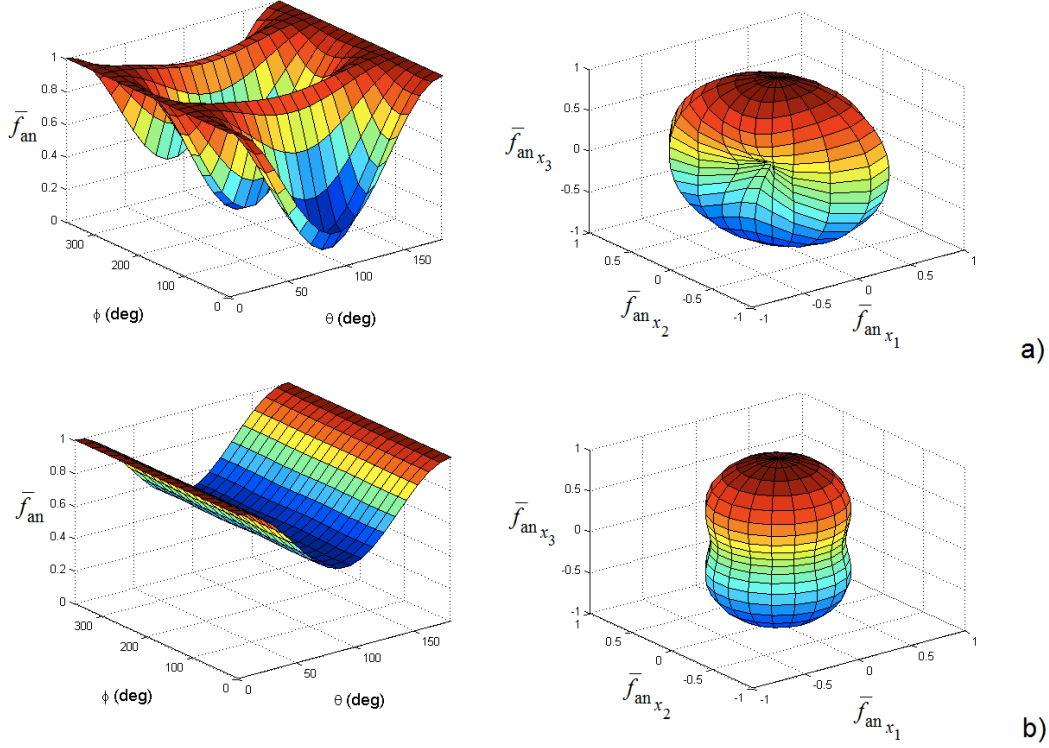


FIGURE 3. Equivalent anisotropy function  $\bar{f}_{\text{an}}(\mathbf{m})$  and corresponding energy surfaces, for Gaussian distribution with  $s = \pi/6$  (a) and for uniform distribution in the film plane (b).

The static hysteresis loop is computed by using a micromagnetic numerical model ([1],[2],[3]). The time evolution towards equilibrium states is calculated by integrating the Landau-Lifshitz-Gilbert (LLG) equation:

$$(5.1) \quad \frac{\partial \mathbf{m}}{\partial t} = -\frac{\gamma G}{(1 + \alpha)^2} [(\mathbf{m} \times \mathbf{H}_{\text{eff}}) + \alpha \mathbf{m} \times (\mathbf{m} \times \mathbf{H}_{\text{eff}})]$$

where  $\gamma G = 2.21 \cdot 10^5 \text{ m A}^{-1} \text{ s}^{-1}$  is the absolute value of the gyromagnetic ratio and  $\alpha$  is the damping constant. The effective field  $\mathbf{H}_{\text{eff}}$  is the sum of the applied field  $\mathbf{H}_a$ , the anisotropy field  $\mathbf{H}_{\text{an}}$ , the exchange field  $\mathbf{H}_{\text{ex}}$  and the magnetostatic field  $\mathbf{H}_m$ . In particular, the exchange field  $\mathbf{H}_{\text{ex}}$  is expressed as:

$$(5.2) \quad \mathbf{H}_{\text{ex}} = \frac{2A}{\mu_0 M_S} \nabla^2 \mathbf{m}$$

being  $A$  the exchange constant of the magnetic material.

The anisotropy field  $\mathbf{H}_{\text{an}}$  is deduced by the anisotropy function  $f_{\text{an}}$  as:

$$(5.3) \quad \mathbf{H}_{\text{an}} = -\frac{1}{\mu_0} \frac{\partial f_{\text{an}}(\mathbf{m})}{\partial \mathbf{m}}.$$

The spatial discretization of the LLG equation is here performed by using first-order finite element shape functions, assuming the Cartesian components of  $\mathbf{m}$  as nodal unknowns [18]. To speed-up the computation and limit the memory requirements, the magnetostatic field due to “far” dipoles is evaluated by a multipole expansion technique [19]. A norm-conserving scheme, based on the Cayley transform ([20] and [21]), is adopted to time integrating the LLG equation, so that the magnitude of  $\mathbf{m}$  is preserved during the time evolution towards equilibrium states.

To compute the descending branch of the static hysteresis loop, the simulation starts from an initially uniform magnetization state pointing in the direction  $x_1$ , then an external field of 200 kA/m is applied along the same direction and reduced in steps of 4 kA/m until the magnetization is reversed. For each step of the applied field, the magnetization time evolution is computed until the equilibrium state, which is assumed to be reached when the maximum nodal value of the misalignment between magnetization and effective field,  $|\mathbf{m} \times \mathbf{H}_{\text{eff}}|$ , is lower than a fixed threshold  $\Theta$ . The optimal values of the time step for the integration of (5.1), as well as the damping constant  $\alpha$  and the threshold  $\Theta$ , have been chosen on the basis of the analysis detailed in [21].

In the simulations here reported, the following physical parameters are considered:  $M_S = 800$  kA/m and  $A = 15$  pJ/m. The magnetic film is discretized into a 2-D mesh with element size  $\sim 6.6$  nm, comparable with the exchange length ( $\sim 6.1$  nm). We assume that  $k_{\text{an}} = 100$  kA/m and anisotropy vector  $\mathbf{u}_{\text{an}}$  is randomly distributed over the film plane ( $x_1x_2$ ), that is  $\theta = \pi/2$ . In Table 1, the values of the fitting parameter  $k_{\text{an}}^*/k_{\text{an}}$  and  $\gamma$ , derived from the homogenization process, are reported, with reference to two limit cases of random distribution. In the first case, we consider a narrow Gaussian distribution ( $s_\phi = \pi/6$ ), that is the easy axis is mainly oriented towards the expected value ( $\eta_\phi = 0$ ), while in the second case a uniform distribution in the film plane is imposed. The corresponding plots of the equivalent anisotropy functions and energy surfaces are shown in Fig. 3.

Case	Interpolating function	$k_{\text{an}}^*/k_{\text{an}}$	$\gamma$
$s_\phi = \pi/6$	(4.4)	0.993	0.796
Uniform distribution	(4.5)	0.5	-1

TABLE 1. Fitting parameters  $k_{\text{an}}^*/k_{\text{an}}$  and  $\gamma$  for Gaussian distribution with  $s_\phi = \pi/6$  and for uniform distribution. The value of  $\eta_\phi$  is fixed to zero.

In Figs. 4 we compare the results of the micromagnetic simulations performed on the magnetic film effectively composed of grains with randomly distributed anisotropy direction  $\mathbf{u}_{\text{an}}$ , with those obtained by considering equivalent homogenized properties. The grain dimension is here fixed to 20 nm. The approximation given by the homogenization approach provides qualitatively good results, leading to hysteresis loops having similar shapes. Anyway, some discrepancies arise in the prediction of the coercive field and of the remanent magnetization. The approximation is strongly influenced by the type of anisotropy random distribution: in particular, with the narrow Gaussian distribution a larger value of the coercive field is found, since the magnetization results much more pinned along the preferential direction. The opposite behavior occurs with a uniform distribution in the film plane, as a consequence of the strong reduction of the equivalent anisotropy constant. Similar results have been found when considering grains having bigger size (100 nm).

#### ACKNOWLEDGMENTS

This work was partially supported by the project GNAMPA 2010 *Problemi variazionali in micromagnetismo* (coordinator: M. Eleuteri). The authors wish to thank Andrey Piatnitski for many helpful suggestions and remarks. The third author is also grateful to the kind hospitality of the Politecnico di Torino and of the INRIM of Torino, where part of the work has been performed, together with the nice and friendly atmosphere there.

#### REFERENCES

- [1] G. Bertotti: *Hysteresis in Magnetism*. Academic Press, 1998.
- [2] H. Kronmüller and M. Fähnle: *Micromagnetism and the Microstructure of Ferromagnetic Solids*. Cambridge University Press, 2003.
- [3] J. Fidler and T. Schrefl: *Micromagnetic modelling-The current state of the art*. J. Phys. D: Appl. Phys. **33** (2000) R135-R156.

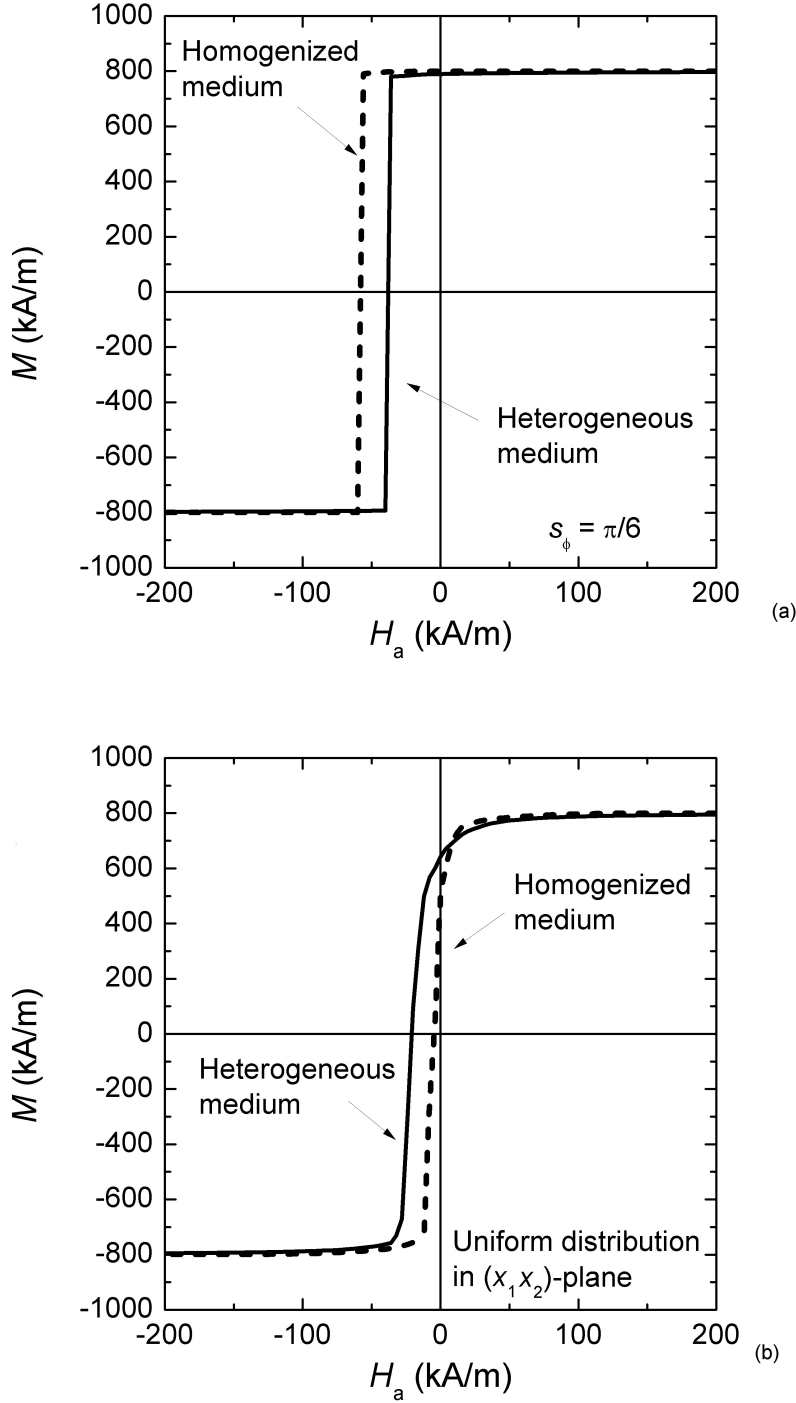


FIGURE 4. Comparison between the descending branches of the static hysteresis loops computed with randomly distributed anisotropy direction (i.e. heterogeneous medium) and with equivalent properties (i.e. homogenized medium): (a) Gaussian distribution with standard deviation  $s_\phi = \pi/6$  and (b) uniform distribution in the film plane. The grain dimension is assumed equal to 20 nm.

- [4] H. Kronmüller, R. Fischer, R. Hertel and T. Leineweber: *Micromagnetism and the microstructure in nanocrystalline materials*. Journal of Magnetism and Magnetic Materials **175** (1997) 177-192.
- [5] J. J. Miles: *Effects of grain size distribution on the performance of perpendicular recording media*. IEEE Trans. Magn. **43** (2007) 955-967.
- [6] J. W. Lau, R. McMichael and M. J. Donahue: *Implementation of two-dimensional polycrystalline grains in object oriented micromagnetics framework*. J. Res. Natl. Inst. Stand. Technol. **144** (2009) 57-67.
- [7] K. M. Tako, M. A. Wongsam and R. W. Chantrell: *Micromagnetics of polycrystalline two-dimensional platelets*. J. Appl. Phys. **79** (1996) 5767-5769.
- [8] K. Z. Gao, J. Fernandez-de-Castro and H. N. Betram: *Micromagnetic study of the switching fields in polycrystalline magnetic thin-film media*. IEEE Trans. Magn. **41** (2005) 4236-4241.
- [9] T. Schrefl, J. Fidler, K. J. Kirk and J. N. Chapman: *Simulation of magnetization reversal in polycrystalline patterned Co elements*. J. Appl. Phys. **85** (1999) 6169-6171.
- [10] Y. M. Jin, Y. U. Wang, A. Kazaryan, Y. Wang, D. E. Laughlin and A. G. Khachaturyan: *Magnetic structure and hysteresis in hard magnetic nanocrystalline film: Computer simulation*. J. Appl. Phys. **92** (2002) 6172-6181.
- [11] K. Piao, D. Li and D. Wei: *The role of short exchange length in the magnetization processes of L10-ordered FePt perpendicular media*. Journal of Magnetism and Magnetic Materials **303** (2006) e39-e43.
- [12] G. Dal Maso: *An Introduction to  $\Gamma$ -convergence*. Birkhäuser, Boston, 1993.
- [13] A. Braides and A. Defranceschi: *Homogenization of multiple integrals*. Oxford University Press, USA, 1998.
- [14] O. Bottauscio, V. Chiadò Piat, M. Eleuteri, L. Lussardi and A. Manzin: *Homogenization of random anisotropy properties in polycrystalline magnetic materials*. Physica B: Condensed Matter (2011), doi:10.1016/j.physb.2011.06.085.
- [15] A. DeSimone, R. V. Kohn, S. Müller and F. Otto: *Recent Analytical Developments in Micromagnetics. The Science of Hysteresis*, eds. G. Bertotti and I. Mayergoyz (Elsevier, 2006) 269-381.
- [16] E. Acerbi, I. Fonseca and G. Mingione: *Existence and regularity for mixtures of micromagnetic materials*. Proc. R. Soc. A **462** (2006) 2225-2243.
- [17] R. D. James and D. Kinderlehrer: *Frustration in ferromagnetic materials*. Continuum Mech. Thermodyn. **6** (1990) 215-239.
- [18] O. Bottauscio, M. Chiampi and A. Manzin: *A finite element procedure for dynamic micromagnetic computations*. IEEE Trans. Magn. **44** (2008) 3149-3152.
- [19] A. Manzin and O. Bottauscio: *A coupled multipole expansion-finite element approach for dynamic micromagnetic modelling*. IEEE Trans. Magn. **45** (2009) 5208-5211.
- [20] D. Lewis and N. Nigam: *Geometric integration on spheres and some interesting applications*. J. Comput. Appl. Math. **151** (2003) 141-170.
- [21] A. Manzin and O. Bottauscio: *Connections between numerical behavior and physical parameters in the micromagnetic computation of static hysteresis loops*. J. Appl. Phys. **108** (2010) 093917.

(O. Bottauscio) ISTITUTO NAZIONALE DI RICERCA METROLOGICA, STR. DELLE CACCE 91, I-10135 TORINO, ITALY.  
 E-mail address: o.bottauscio@inrim.it  
 URL: <http://www.inrim.it/~botta/>

(V. Chiadò Piat) POLITECNICO DI TORINO, C.SO DUCA DEGLI ABRUZZI 24, I-10129 TORINO, ITALY.  
 E-mail address: valeria.chiadopiat@polito.it

(M. Eleuteri) UNIVERSITÀ DI TRENTO, VIA SOMMARIVE 14, I-38100 POVO (TRENTO), ITALY.  
 E-mail address: eleuteri@science.unitn.it  
 URL: <http://www.science.unitn.it/~eleuteri/>

(L. Lussardi) UNIVERSITÀ CATTOLICA DEL SACRO CUORE, VIA DEI MUSEI 41, I-25121 BRESCIA, ITALY.  
 E-mail address: l.lussardi@dmf.unicatt.it  
 URL: <http://www.dmf.unicatt.it/~lussardi/>

(A. Manzin) ISTITUTO NAZIONALE DI RICERCA METROLOGICA, STR. DELLE CACCE 91, I-10135 TORINO, ITALY.  
 E-mail address: a.manzin@inrim.it